EPJ Web of Conferences **171**, 01002 (2018) https://doi.org/10.1051/epjconf/201817101002
SQM 2017

News from the NA61/SHINE experiment

Tatjana Šuša for the NA61/SHINE Collaboration[1,⋆]

[1] *Institute Ruđer Bošković*

Abstract. The main goals of the NA61/SHINE experiment at the CERN SPS are the search for the critical point of strongly interacting matter and the study of the properties of the onset of deconfinement. These aims are pursued by performing a two-dimensional scan of the phase diagram of strongly interacting matter by varying the momentum and size of the colliding nuclei.
This contribution summarises the latest results from the NA61/SHINE experiment, in particular, new results on spectra and yields of ϕ meson in p+p interactions at 40, 80 and 158 GeV/c and K^+ and K^- production in central Be+Be collisions at mid-rapidity. In addition, results on system size dependence of particle yield ratios and fluctuations are presented.

1 Introduction

NA61/SHINE [1] is a fixed-target experiment located in the H2 beam line of the CERN SPS accelerator complex. The main detector system is a set of five Time Projection Chambers (TPCs) which allows a precise measurement of the particle momenta and provides particle identification via the measurement of the specific energy loss, dE/dx. Two time-of-flight walls improve the kaon identification capabilities. The geometrical layout of the TPCs allows particle detection down to $p_T = 0$ GeV/c in a broad interval of forward rapidities. A high resolution hadron calorimeter, the Projectile Spectator Detector, measures forward going energy E_F and is used to select centrality in nuclear collisions.

The main goal of the strong interactions programme of the NA61/SHINE experiment is to discover the critical point of strongly interacting matter and study the properties of the onset of deconfinement. The programme is motivated by the discovery of the onset of deconfinement in Pb+Pb collisions at 30A GeV/c by the NA49 experiment [2, 3]. To achieve this goal a two-dimensional scan of the phase diagram of strongly interactiong matter is performed by varying the beam momentum (13A-150/158A GeV/c) and the size of the colliding nuclei (p+p, p+Pb, Be+Be, Ar+Sc, Xe+La, Pb+Pb).

2 Recent results from NA61

2.1 ϕ meson production in p+p interactions

The production of ϕ meson is measured in p+p interactions at 40, 80 and 158 GeV/c. ϕ mesons were identified by their charged kaon decays $\phi \rightarrow K^+K^-$ using the invariant mass method. The statistics

⋆e-mail: tatjana.susa@irb.hr

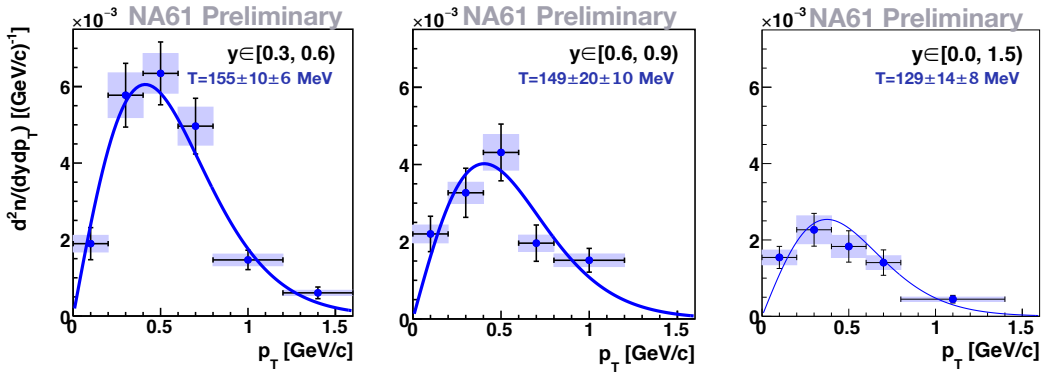

Figure 1. Examples of transverse momentum distributions of ϕ mesons in p+p interactions at beam momenta of 158 (left), 80 (middle) and 40 (right) GeV/c.

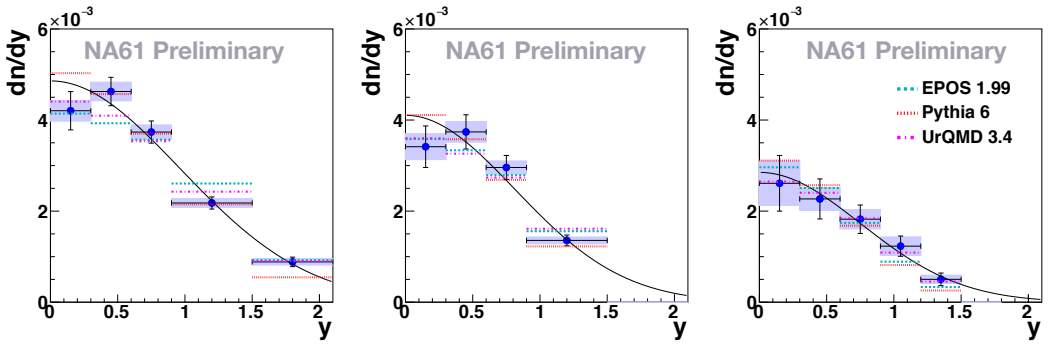

Figure 2. Rapidity distributions of ϕ mesons in p+p interactions at beam momenta od 158 (left), 80 (middle) and 40 (right) GeV/c.

of 40 GeV/c dataset only allowed to extract single differential dn/dy and dn/dp_T spectra in one wide transverse momentum ($p_T \in [0, 1.4]$ GeV/c) and one rapidity ($y \in [0, 1.5]$) bin, respectively, while at 80 and 158 GeV/c a double-differential analysis in bins of rapidity and transverse momentum could be performed. These are the first measurements of ϕ production at 40 and 80 GeV/c and the first double-differential measurements at 158 GeV/c.

Examples of p_T spectra are presented in Fig. 1. The systematic uncertainties are shown by the blue shaded boxes while horizontal error bars indicate the width of the p_T bins. The spectra are fitted with an exponential function in m_T shown by the blue curve. The extracted values of the inverse slope parameter T at 80 and 158 GeV/c are in the range 120 - 160 MeV and decrease with increasing rapidity (see conference slides).

The rapidity spectra of ϕ mesons are presented in Fig. 2. The systematic uncertainties are shown by the blue shaded boxes while horizontal error bars indicate the width of the rapidity bins. Shown are also predictions for the shape of rapidity spectra from the Epos1.99 [4, 5] (version in CRMC1.6.0 package [6]), Pythia6.4.28 [7] and Urqmd3.4 [8, 9] models which are normalised to the integral of the data. All models approximately describe the shape of the spectra. The result of the fit with a single Gaussian to the experimental points is shown by the black curve. The width of the rapidity spectra

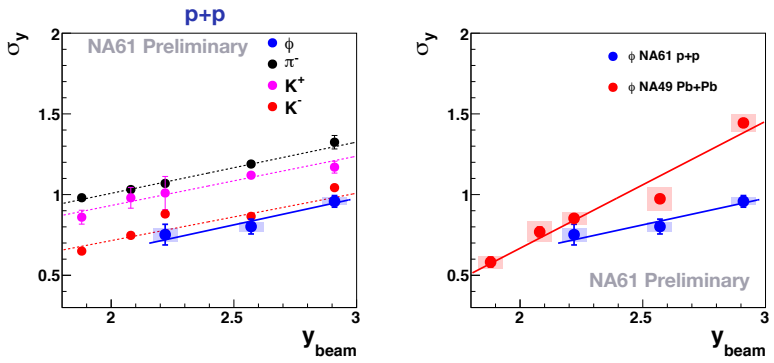

Figure 3. Width of the rapidity distributions of ϕ, π^- and $K^\pm$ mesons in p+p collisions (left), width of the rapidity distributions of ϕ mesons in p+p and Pb+Pb collisions (right) as a function of beam rapidity.

derived from the fit is compared to the width of the rapidity spectra of π^-, K^+ and K^- in p+p [10] collisions in Fig. 3 (left) and to the width of the rapidity spectra of ϕ meson in Pb+Pb [11] collisions in Fig. 3 (right). While in p+p collisions the ϕ follows the trend of the other hadrons, the widths of the rapidity distributions of ϕ mesons in p+p and Pb+Pb exhibit different behavior.

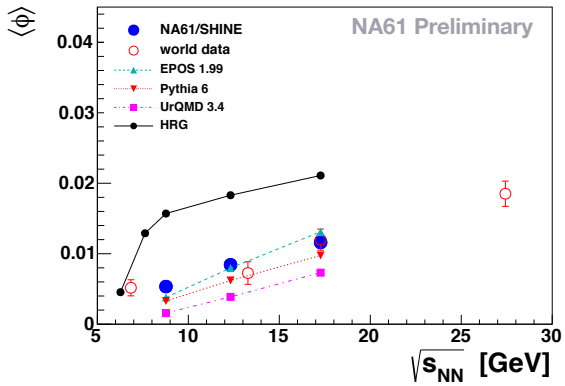

Figure 4. Energy dependence of the mean ϕ multiplicity in p+p collisions, together with the data from other experiments [12–15] and predictions from Epos1.99 [4, 5], Pythia6.4.28 [7], UrQMD3.4 [8, 9] and HRG [16] models.

The mean ϕ multiplicity, $\langle\phi\rangle$, is derived by summing the measured rapidity spectra and by extrapolation to the unmeasured high rapidity region using the fitted single Gaussian. The obtained values are doubled to take into account the contribution from the backward hemisphere. The NA61 results on mean ϕ multiplicity are compared in Fig. 4 to the world data [12–15] and to the predictions of the Epos, Pythia6, UrQMD and hadron resonance gas (HRG [16]) models. The NA61/SHINE results on mean ϕ multiplicity are consistent with the world data and are much more accurate. The Epos model describes the data quite well, Pythia6 underestimates the experimental data, while UrQMD underestimates and HRG overestimates NA61/SHINE results approximately by a factor two.

The ratio of mean multiplicity of ϕ mesons and pions in p+p and central Pb+Pb collisions as a function of center of mass energy per nucleon pair is shown in Fig. 5 (left), while the double ratio (Pb+Pb)/(p+p) of the ratios $\langle\phi\rangle/\langle\pi\rangle$ and $\langle K^\pm\rangle/\langle\pi^\pm\rangle$ is presented in Fig. 5 (right). Pb+Pb data are from NA49 [2, 3, 11], while p+p kaon and pion data are taken from Ref. [10]. As seen from Fig. 5 (left) the $\langle\phi\rangle/\langle\pi\rangle$ ratio increases with $\sqrt{s_{NN}}$. In Pb+Pb collisions it is approximately three times larger than in p+p collisions, independently of the interaction energy. Figure 5 (right) shows that the enhancement between pp and PbPb of the double ratio $\langle\phi\rangle/\langle\pi\rangle$ is close to that of $\langle K^+\rangle/\langle\pi^+\rangle$ and systematically larger than that of $\langle K^-\rangle/\langle\pi^-\rangle$.

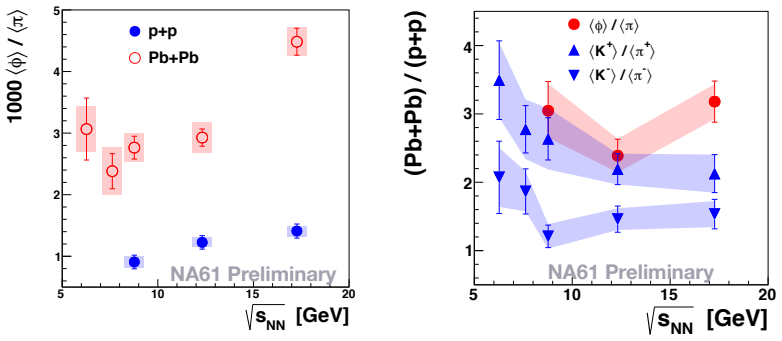

Figure 5. Energy dependence of the $\langle\phi\rangle/\langle\pi\rangle$ ratio in p+p and central Pb+Pb collisions (left) and the double (Pb+Pb)/(p+p) ratio of the $\langle\phi\rangle/\langle\pi\rangle$ and $\langle K^{\pm}\rangle/\langle\pi^{\pm}\rangle$ ratios (see text for references).

2.2 Kaon production in Be+Be interactions

NA61/SHINE performed the first measurement of $K^{\pm}$ production at mid-rapidity in the most violent Be+Be interactions (the 20% of events with the smallest forward energy, E_F) at 30A, 40A, 75A and 150A GeV/c. The $K^{\pm}$ mesons were identified based on the measurement of the energy loss in the TPCs (dE/dx) and time-of-flight in the ToF detectors.

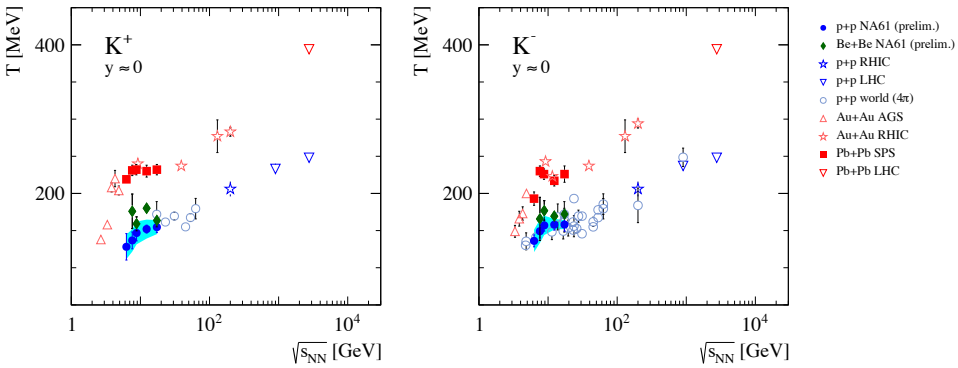

Figure 6. Energy dependence of the inverse slope parameter of m_T spectra at mid-rapidity of positively (left) and negatively (right) charged kaons.

Fig. 6 and Fig. 7 present the energy dependence of the inverse slope parameter of m_T spectra of charged kaons and the multiplicity ratio of charged kaons to pions at mid-rapidity, respectively. Results for Be+Be interactions are compared with NA61/SHINE p+p results and with results from central Pb+Pb collisions from NA49 [2, 3] and other experiments [17–24]. A plateau in the energy dependence of the inverse slope parameter and a peak observed in the energy dependence of the multiplicity ratio of charged kaons to pions in Pb+Pb collisions were predicted by the SMES [25] model as signatures of the onset of deconfinement. The NA61/SHINE results on the energy dependence of the inverse slope parameter in p+p and Be+Be interactions are also consistent with the plateau in the SPS energy range, while a step structure with plateau is observed in the energy dependence of the K^+/π^+ ratio, suggesting that some properties of hadron production previously attributed to onset of deconfinement in heavy ion collisions might be present also in p+p and Be+Be interactions.

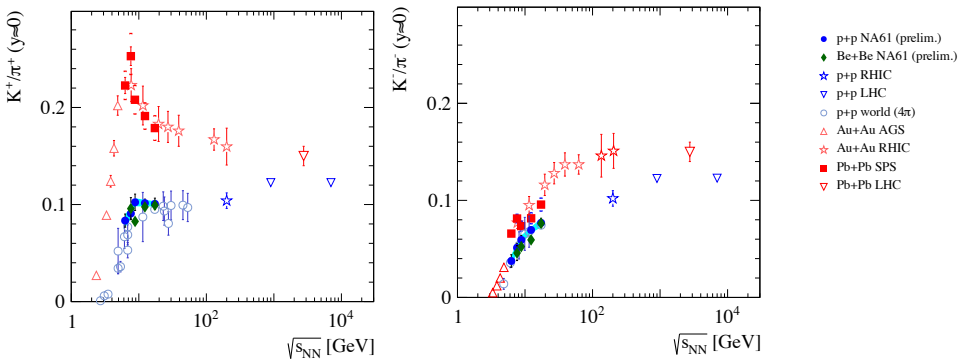

Figure 7. Energy dependence of the ratio of positively (left) and negatively (right) charged kaon to pion yield at mid-rapidity.

2.3 System size dependence of particle yields and fluctuations

NA61/SHINE results on the system size dependence of particle yield ratios and fluctuations are presented in Fig. 8 and Fig. 9, respectively.

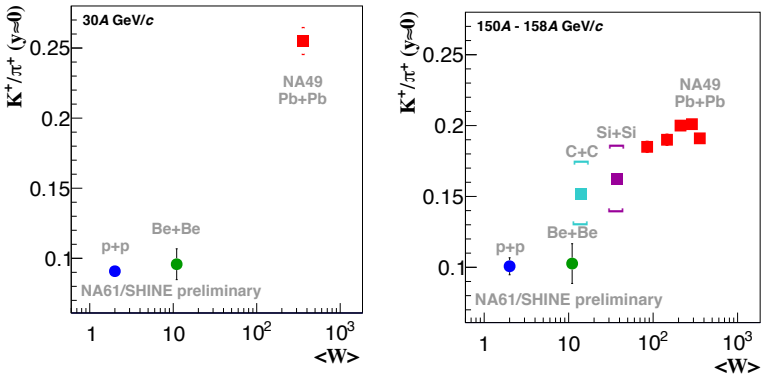

Figure 8. Ratio of positively charged kaon to pion yield at mid-rapidity as a function of mean number of wounded nucleons $\langle W \rangle$ at 30A (left) and 150/158A (right) GeV/c.

In Fig. 8 the ratios of positively charged kaon to pion yield at mid-rapidity in p+p and Be+Be collision at 30A and 150/158A GeV/c are shown, together with the C+C, Si+Si and Pb+Pb data from the NA49 experiment. Mid-rapidity K^+/π^+ ratios in p+p and Be+Be collisions are very close, independently of the collison energy and differ significanty from those in medium and heavy system.

NA61/SHINE uses the scaled variance of the multiplicity distribution $\omega[N] \equiv Var(N)/\langle N \rangle$ to characterize the strength of multiplicity fluctuations. It is an intensive variable, insensitive to the volume of the system, but sensitive to fluctuations of the volume. In Fig. 9 the scaled variance of the multiplicity distribution of negatively charged hadrons in p+p, Be+Be and Ar+Sc collisions at 30A and 150/158 AGeV/c is shown as a function of the mean number of wounded nucleons $\langle W \rangle$.

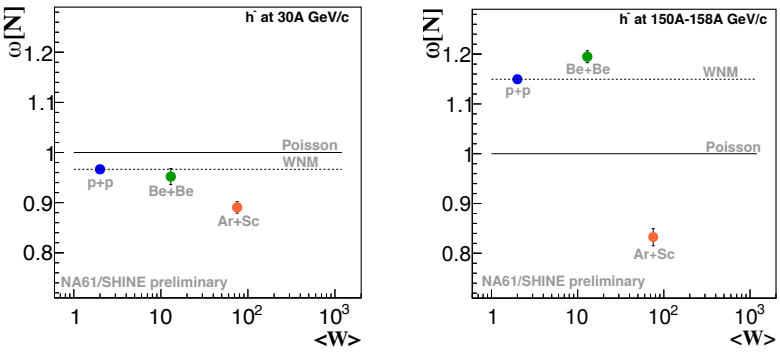

Figure 9. The scaled variance of the multiplicity distribution of negatively charged hadrons in p+p, Be+Be and Ar+Sc collisions at 30A (left) and 150/158A (right) GeV/c as a function of the mean number of wounded nucleons $\langle W \rangle$.

The multiplicity fluctuations in p+p and Be+Be collisions are similar and significantly higher than in Ar+Sc collisions. The observed suppression of the scaled variance in Ar+Sc collisions is not expected for an Ideal Boltzmann gas in the Grand Canonical Ensamble treatment nor in the Wounded Nucleon Model [26].

References

[1] N. Abgrall et al., JINST **9**, P06005 (2014)
[2] C. Alt et al., Phys. Rev. C**77**, 024903 (2008)
[3] S. V. Afanasiev et al., Phys. Rev. C**66**, 054902 (2002)
[4] K. Werner, F. Liu, and T. Pierog, Phys. Rev. C**74**, 044902 (2006)
[5] T. Pierog and K. Werner, Nucl. Phys. B (Proc. Suppl.) **196**, 102 (2009)
[6] C. Baus, T. Pierog, and R. Ulrich, https://web.ikp.kit.edu/rulrich/crmc.html
[7] T. Sjöstrand, S. Mrenna, and P. Skands, J. High Energy Phys. **05**, 026 (2006)
[8] S. Bass et al., Prog. Part. Nucl. Phys. **41**, 255 (1998)
[9] M. Bleicher et al., J. Phys. G**25**, 1859 (1999)
[10] S. Pulawski, PoS CPOD **2014**, 010 (2015)
[11] C. Alt et al., Phys. Rev. C**78**, 044907 (2008)
[12] V. Blobel et al., Phys. Lett. B**59**, 88 (1975)
[13] C. Daum et al., Nucl. Phys. B**186**, 205 (1981)
[14] Aguilar-Benitez et al., Z. Phys. C**50**, 405 (1991)
[15] S. Afanasiev et al., Phys. Lett. B**491**, 59 (2000)
[16] V. Vovchenko, V. V. Begun, M. I. Gorenstein, Phys. Rev. C**93**, 064906 (2016)
[17] M. Gazdzicki, D. Roehrich, Z. Phys. C**65**, 215 (1995)
[18] M. Gazdzicki, D. Roehrich, Z. Phys. C**71**, 55 (1996)
[19] M. Kliemant, B. Lungwitz, M. Gazdzicki, Phys. Rev. C**69**, 044903 (2004)
[20] I. Arsene et al., Phys. Rev. C**72**, 014908 (2005)
[21] K. Aamodt et al., Eur. Phys. J. C**71**, 1655 (2011)
[22] B. Abelev et al., Phys. Rev. C**79**, 034909 (2009)
[23] B. Abelev et al., Phys. Lett. B**736**, 196 (2014)
[24] B. Abelev et al., Phys. Rev. Lett. **109**, (2012)
[25] M. Gazdzicki, M. I. Gorenstein, Acta Phys. Polon. B**30**, 2705 (1999)
[26] A. Bialas, M. Bleszynski and W. Czyz, Nucl. Phys. B**111**, 461 (1976)